Journal of Molecular Catalysis A: Chemical 327 (2010) 92–100

Contents lists available at ScienceDirect

Journal of Molecular Catalysis A: Chemical

journal homepage: www.elsevier.com/locate/molcata

A strategy to immobilize noble metal nanoparticles on silica microspheres

Shengnan Wang, Minchao Zhang, Luwei Zhong, Wangqing Zhang*

Key Laboratory of Functional Polymer Materials of Ministry of Education, Institute of Polymer Chemistry, Nankai University, Tianjin 300071, China

ARTICLE INFO

Article history:
Received 12 March 2010
Received in revised form 7 May 2010
Accepted 26 May 2010
Available online 1 June 2010

Keywords:
Silica microspheres
Pd nanoparticles
Immobilized catalyst
Dispersion polymerization

ABSTRACT

A strategy to immobilize noble metal nanoparticles on silica microspheres is proposed. Following this strategy, 350 nm silica microspheres synthesized by Stöber method are initially activated with 3-(trimethoxysilyl) propyl methacrylate to anchor C=C bonds on the surface of the silica microspheres. Then a thin layer of coordination polymer containing chelate ligand of β-diketone is coated on the surface of the activated silica microspheres by dispersion polymerization. The noble metal nanoparticles therefore can be immobilized on the polymer coated silica microspheres initially through coordination between the chelate ligand of β-diketone in the coating polymer and the metal precursors followed by reduction. It is found that 5.1 nm Pd, 6.1 nm Au, and 5.7 nm Ag nanoparticles can be immobilized on the polymer coated silica microspheres. The typical immobilized Pd catalyst is tested using hydrogenation of cinnamyl alcohol in water at 300 K as model reaction. The catalysis demonstrates that the immobilized Pd catalyst affords a turnover frequency of 270 h^{-1} with minimal leaching and it could be recycled ~8 times without any loss of activity.

1. Introduction

Catalytically active noble metal nanoparticles immobilized on a suitable support or scaffold have been widely used in various chemical conversions [1]. It is generally deemed that the catalyst support is a critical factor that affects the catalytic performance including activity and selectivity of noble metal nanoparticles [2,3]. Besides, immobilization of noble metal nanoparticles on suitable support can prevent agglomeration and facilitate catalyst recycling [1]. Consequently, various supports such as organic polymeric materials [4–6], inorganic materials [7–11], and organic/inorganic hybrid materials [12–15] have been employed as scaffold for noble metal nanoparticles. Generally, two features should be of concern when employing a material as catalyst support. First, the material should be both thermally and chemically stable during the catalysis. Second, the structure of the support has to be such that the catalytically active sites are well dispersed on its surface and these sites are easily accessible. Of all the supporting materials, silica appears to be candidate due to its stability, high surface area, easily tunability and economic availability [16–18]. The noble metal nanoparticles immobilized on silica materials have been extensively studied as catalysts over the last decade in various chemical reactions including oxidation, hydrogenation, hydrochlorination, C–C coupling reaction and so on [16–19].

The methodology of immobilization of noble metal nanoparticles on silica materials mainly includes physicochemical routes and chemical processes. In physicochemical processes, which mainly includes ion-exchange [20,21], incipient wetness impregnation [22,23], encapsulation [24,25], and organometallic methodology [26–28], noble metal nanoparticles are deposited on the surface of or incorporated in silica by means of electrostatic, chemical or biochemical interaction without modifying the structure of the supporting material. For examples, Ichikawa and co-workers initially employed the impregnation method, followed a mild UV–vis-irradiation-based reducing process to immobilize Pt or Au nanoparticles within the silica materials, by which the diffusion of metal ions at high temperature process was avoided [22]. With the *in situ* encapsulation method, Devi and co-workers declared that the anionic metal precursor of H_2PtCl_6 could be incorporated within the surfactant micelles of CTAB during the synthesis of mesoporous silica materials [25]. Upon further thermal treatment, Pt nanoparticles could be obtained and incorporated within the mesoporous silica. Johnston et al. [29] and Rioux et al. [30] found that the dodecanethiol-stabilized Au nanoparticles and the polyvinylpyrrolidone-coated Pt nanoparticles could be infused into mesoporous silica with the help of supercritical CO_2 or by sonication. Since organometallic complexes or clusters are highly active towards silanols, Anderson and co-workers found that the organometallic complex precursors could be introduced into the channels of mesoporous silica by covalent bonding [26]. However, due to the relatively weak interaction between noble metal nanoparticles/metal precursor and silica, in general, it is difficult to immobilize metal nanoparticles on/within silica materials in a con-

* Corresponding author. Tel.: +86 22 23509794; fax: +86 22 23503510.
E-mail address: wqzhang@nankai.edu.cn (W. Zhang).

1381-1169/$ – see front matter © 2010 Elsevier B.V. All rights reserved.
doi:10.1016/j.molcata.2010.05.018

trolled fashion simply by impregnating or ion-exchange. However, in chemical processes, the silica materials are initially functionalized with appropriate ligand such as thiol or amino group and then noble metal nanoparticles are immobilized [31–36]. For instance, Corriu and co-workers [31] grafted thiol group on the surface of silica, and then Au ions were immobilized within the mesoporous silica initially through the strong metal–sulfur complexation followed by a solution reducing process. Shi and co-workers [36] developed a novel *in situ* reducing route for selective encapsulation of metal nanocomposites within mesoporous SBA-15. Following this method, the silanol group on the outer surface of the as-synthesized SBA-15 was modified initially with the methyl group followed by a series of anhydrous organic reactions to give the reducing Si–H functional group. After introducing the metal precursors (e.g., H_2PtCl_6 or H_2PdCl_6), Pd nanoparticles or Pt nanowires were synthesized within the channels of SBA-15.

Coating methodology is widely used to modify surface of particles. Polymerization on silica affords a valid method to form polymer coated silica materials. Up to now, various polymer coated silica materials such as silica/polymer core–shell particles [37–41] and silica/polymer composites [42,43] have been fabricated. For example, Yang and co-workers have prepared silica/polymer core–shell particles by emulsion polymerization of styrene employing 3-(trimethoxysilyl) propyl methacrylate-grafted silica nanoparticles as seed [40]. Atkin and co-workers have reported the coating of poly(vinylpyridine) on poly(vinylpyridine)-microgel-adsorbed-silica particles by seed polymerization to form silica/polymer core–shell particles [41]. Due to the relatively easy modification of polymer, the polymer coating methodology provides great potential to immobilize noble metal nanoparticles on silica materials.

Herein, a simple and valid strategy to immobilize noble metal nanoparticles on silica microspheres is proposed. Initially, monodispersed silica microspheres are synthesized by Stöber method [44]. Then, the resultant silica microspheres are coated with a thin layer of chelate polymer of poly[styrene-*co*-2-(acetoacetoxy) ethyl methacrylate] (PS-*co*-PAEMA) by dispersion polymerization [45] and thus the polymer coated silica microspheres of silica@polymer are produced. Finally, Pd, Au or Ag nanoparticles are immobilized on the silica@polymer microspheres initially through coordination between the metal precursor and the chelate ligand of β-diketone in the coated polymer layer followed by reduction with $NaBH_4$ aqueous solution. The typical catalyst of the immobilized Pd nanoparticles is tested by employing the hydrogenation of cinnamyl alcohol in water as model reaction. It is demonstrated that the catalyst of Pd nanoparticles immobilized on the polymer coated silica microspheres of silica@polymer is stable, efficient and reusable.

2. Experimental

2.1. Materials

Styrene (St, >98%, Tianjin Chemical Company) was distilled under vacuum before being used. Divinylbenzene (DVB, >80%, Alfa Aesar) was washed initially with 5% NaOH aqueous solution and then deionized water followed drying with $MgSO_4$. Azobisisobutyronitrile (AIBN, >99%, Tianjin Chemical Company) was recrystallized from acetone before being used. The monomer of 2-(acetoacetoxy) ethyl methacrylate (AEMA, >95%, Aldrich), 3-(trimethoxysilyl) propyl methacrylate (MPS, >99%, Alfa Aesar), cinnamyl alcohol (>99%, Shanghai Shuangxi Spice Assistant Co., Ltd.), $PdCl_2$ (>99%, Alfa Aesar), tetraethylorthosilicate (TEOS, >99%, Alfa Aesar), ammonium hydroxide (25 wt% aqueous solution, Tianjin Chemical Company), polyvinylpyrrolidone (PVP, average molecular weight 10,000D, Tianjin Chemical Company), $NaBH_4$ (>98.9%, Tianjin Chemical Company) and other analytical reagents were used as received.

2.2. Preparation of silica microspheres

Silica microspheres were fabricated by following the Stöber method [44]. In a typical procedure, 0.040 mol of TEOS (8.334 g) was added into 208 mL of the mixture of ethanol, water and 25 wt% ammonia aqueous solution (180/20/8 by volume). The hydrolysis of TEOS was maintained at room temperature for 12 h with vigorous stirring. Aliquot dispersion of the resultant silica microspheres was used to synthesize polymer coated silica microspheres of silica@polymer, and the other was isolated by centrifugation, washed initially with mixture of ethanol and water (9:1 by volume) and then with water, and finally dispersed in water for the next use.

2.3. Preparation of polymer coated silica microspheres of silica@polymer

Into a flask the resultant dispersion of the silica microspheres (104 mL, containing 0.020 mol of Si) and MPS (1.5 mmol) were added. The dispersion was kept at room temperature for 12 h with vigorous stirring. The resultant MPS-activated silica microspheres were collected by centrifugation and then dispersed in 100 mL of ethanol and water (9:1 by volume) containing the stabilizer PVP (0.180 g). Subsequently, the mixture of styrene (0.393 g, 3.77 mmol), AEMA (0.808 g, 3.77 mmol) and DVB (0.049 g, 0.38 mmol) was added dropwise with vigorous stirring. The flask content was purged with nitrogen at room temperature, and then AIBN (0.062 g, 0.38 mmol) was added. The flask content was purged again, and polymerization was performed at 70 °C for 24 h under nitrogen atmosphere with vigorous stirring. Finally, the product of the polymer coated silica microspheres of silica@polymer was initially purified by centrifugation and then dispersed in 50.0 mL of water for next use. The silica concentration in the aqueous dispersion was 0.40 mmol/mL.

2.4. Immobilization of noble metal nanoparticles on silica@polymer microspheres and silica microspheres

To immobilize noble metal nanoparticles on silica@polymer microspheres, a given volume of 5.0 mmol/L aqueous solution of the metal precursor ($PdCl_2$, $HAuCl_4$ or $AgNO_3$) was added into the aqueous dispersion of the silica@polymer microspheres (5.0 mL, 0.40 mmol/mL). The mixture was initially kept in ice water for 2 h with stirring and then the pH value was adjusted to ~7 with NaOH aqueous solution. Subsequently, cool $NaBH_4$ aqueous solution (9.4 mL, 20.0 mmol/L) was added dropwise with vigorous stirring. The final dispersion of the noble metal nanoparticles immobilized on silica@polymer microspheres (Pd/silica@polymer, Au/silica@polymer or Ag/silica@polymer) was dialyzed against water and then dispersed in a given volume of water.

The immobilization of Pd nanoparticles on silica microspheres without coated polymer was same as those on the silica@polymer microspheres except that silica microspheres were employed.

2.5. Catalyst testing

2.5.1. General procedures for hydrogenation

Herein, the typical catalyst of Pd/silica@polymer was tested by employing the hydrogenation of cinnamyl alcohol in water as model reaction. Cinnamyl alcohol (2.0 mmol), the aqueous dispersion of the Pd/silica@polymer catalyst (4.0 mL, containing 4.0×10^{-3} mmol Pd), and 11.0 mL of water were added into a 100 mL tube-like glass reactor equipped with a reflux condenser.

Hydrogenation was performed at 27 °C (300 K) by bubbling H_2 (0.01 L/min) at atmospheric pressure. The hydrogenation was monitored with ^{1}H NMR (see details in Supporting Information). For ^{1}H NMR analysis, the withdrawn aqueous dispersion was initially extracted with $CHCl_3$, and subsequently the collected organic phase was concentrated, and the resultant solid was dried under vacuum at room temperature, and then dissolved in $CDCl_3$.

2.5.2. Catalyst leaching

To detect Pd leaching from the Pd/silica@polymer catalyst into aqueous phase, after 1 h of hydrogenation at 27 °C, the reaction mixture was initially filtered at the reaction temperature and then the filtrate was collected. The filtrate was further bubbled with H_2 at 27 °C and the hydrogenation was monitored with ^{1}H NMR. After the hydrogenation was stopped, the filtrate was analyzed with atomic absorption spectroscopy (AAS) to detect Pd catalyst.

2.5.3. Catalyst reuse

After the hydrogenation of cinnamyl alcohol was just completed in 2.5 h, the Pd/silica@polymer catalyst, which existed as very fine precipitate in the bottom of the tube-like glass reactor, was collected, and the decanted aqueous phase was analyzed with ^{1}H NMR. The same amount of cinnamyl alcohol (2.0 mmol) and water (15.0 mL) were re-loaded into the tube-like glass reactor and the next run of hydrogenation was started at 27 °C by bubbling H_2 for 2.5 h as the fresh run of hydrogenation. To diagnose possible aggregation of the immobilized Pd nanoparticles, the aqueous dispersion of the recycled catalyst was detected by transmission electron microscopy (TEM). To detect the Pd content in the recycled Pd/silica@polymer catalyst, AAS analysis was applied.

2.6. Characterization

TEM observation was conducted by using a Philips T20ST electron microscope at an acceleration voltage of 200 kV, whereby a small drop of the sample was deposited onto a carbon-coating copper grid and dried at room temperature under atmospheric pressure. Fourier-transform infrared (FT-IR) measurement was performed on a Bio-Rad FTS-6000 IR spectrometer using KBr pellets. The thermogravimetric analysis (TGA) was performed on a thermogravimetric analyzer (TG 209, NETZSCH) under nitrogen, with a heating rate of 10 °C/min. The ^{1}H NMR spectra were recorded on a UNITY PLUS-400 spectrometer using $CDCl_3$ as solvent. The solid state ^{13}C NMR measurement was performed on a Varian Infinity-plus wide-bore (89 mm) NMR spectrometer at spin rate of 13 kHz, which was equipped with a double-resonance HX CP/MAS probe. The powder X-ray diffraction (XRD) measurement was performed on a Rigaku D/max 2500 X-ray diffractometer. To get solid sample for XRD analysis, the aqueous dispersion of the noble metal nanoparticles immobilized on silica@polymer microspheres was first freeze-dried and then characterized with XRD. AAS analysis was performed on a Solaar AAS 2 atomic absorption spectrometer.

3. Results and discussion

3.1. Synthesis and characterization of the polymer coated silica microspheres of silica@polymer

Scheme 1 schematically shows the strategy to immobilize Pd nanoparticles on the polymer coated silica microspheres of silica@polymer. First, silica microspheres are synthesized by Stöber method [44]. Second, the silica microspheres are activated with MPS to anchor C=C bond on the surface of the silica microspheres. It is generally deemed that the hydroxy group (–OH) on the surface of silica can form complexes with the $(CH_3O)_3$–Si group [37–40] and therefore produce MPS-activated silica microspheres.

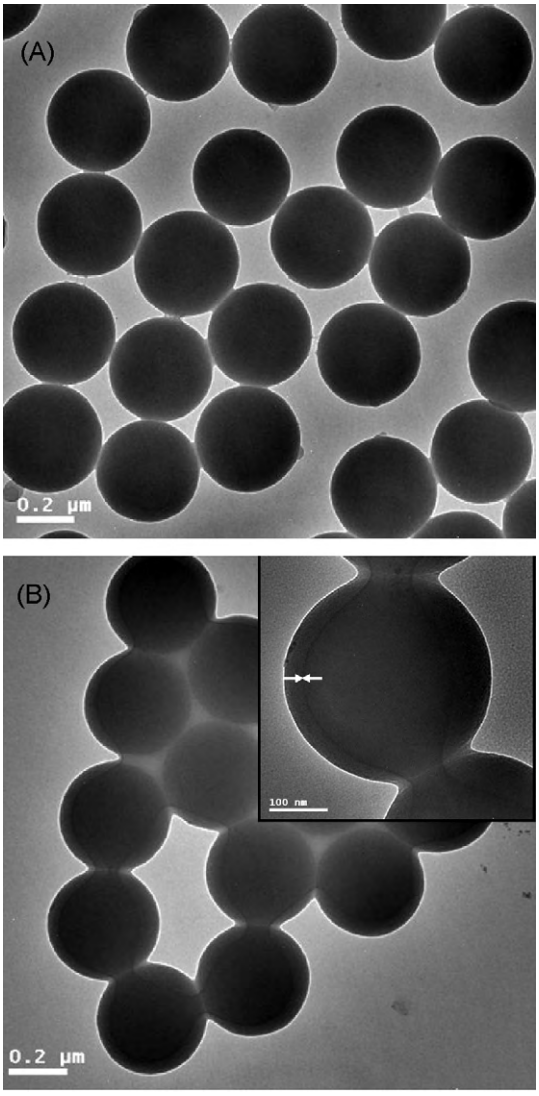

Fig. 1. The TEM images of the silica microspheres (A) and the polymer coated silica microspheres of silica@polymer (B).

Due to the anchored C=C bond and the hydrophobic surface of the MPS-activated silica microspheres, polymer coating on silica microspheres can be achieved by dispersion polymerization [45] of styrene and AEME in the presence of 5.0 mol% cross-linker of DVB employing PVP as stabilizer, and therefore the polymer coated silica microspheres of silica@polymer are produced. In the thin coated polymer layer, the PAEME segment is used to immobilize noble metal nanoparticles since it contains chelate ligand of β-diketone [46–48]. The PS segment is introduced to increase the thermal stability of the coated polymer layer since the glass transition temperature (T_g) of the PAEMA segment is very low (~3 °C) [48]. Finally, the noble metal nanoparticles are immobilized on the polymer coated silica microspheres initially through coordination between the β-diketone ligand and the metal precursor followed by reduction with $NaBH_4$ aqueous solution. Herein, it should be pointed out that the coated polymer is resulted from the copolymerization of styrene, AEMA, and the cross-linker DVB with MPS, which is anchored on the surface of silica microspheres, therefore the coated polymer is deemed to be covalently bonded rather than simply physisorbed on the silica microspheres.

Fig. 1A shows the TEM image of the silica microspheres, indicating that the silica microspheres have a smooth surface. Clearly, the size of the silica microspheres is almost monodispersed and the

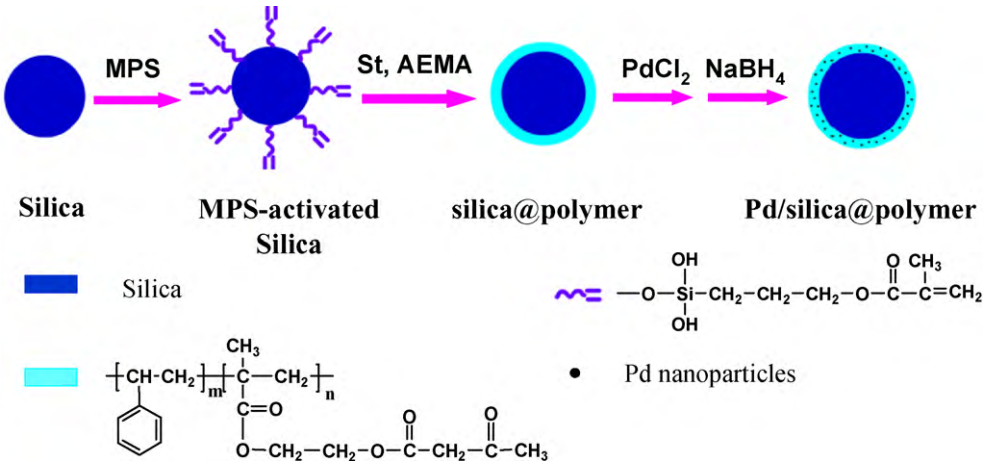

Scheme 1. Schematic synthesis of Pd nanoparticles immobilized on the silica@polymer microspheres.

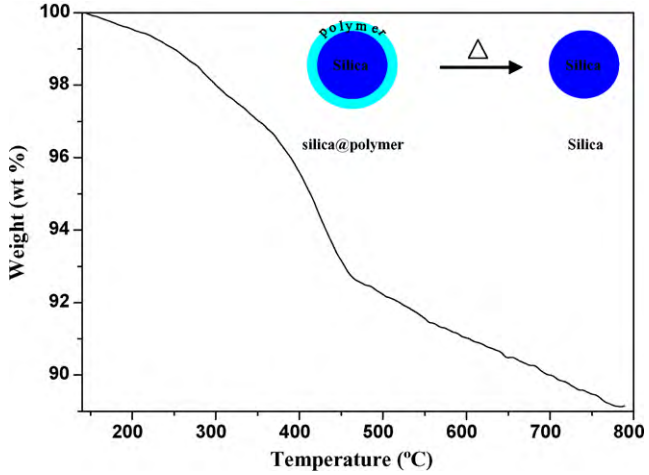

Fig. 2. TGA curve of the silica@polymer microspheres.

average diameter is about 350 nm. Fig. 1B shows the TEM image of the polymer coated silica microspheres of silica@polymer. Compared with Fig. 1A, a thin polymer layer with average thickness of ~15 nm is clearly observed in Fig. 1B, indicating that the polymer has been coated onto the silica microspheres.

TGA is widely used to determine the composition of inorganic/organic hybrid materials [15,49]. When heated above a critical temperature, the organic content in the hybrid material will be decomposed and the inorganic content will be held as schematically shown in the inset in Fig. 2. Herein, TGA is employed to detect the polymer content in the polymer coated silica microspheres of silica@polymer. As shown in Fig. 2, ~3.5% weight loss can be observed when the polymer coated silica microspheres are heated by increasing temperature from 100 to 380 °C, suggesting that the polymer content in the silica@polymer microspheres is about 3.5 wt%. Assuming that the weight density of the silica microspheres and the coating polymer layer are 2.2 [50] and 1.0 g/cm^3, respectively, the thickness of the coating polymer layer in the silica@polymer microspheres is calculated to be 5 nm, which is smaller than those observed by TEM as shown in Fig. 1B. The reason is possibly ascribed to the low T_g of the PAEMA segment [48], which makes the coated polymer somewhat molten during the TEM observation and therefore high thickness of the coated polymer layer in the silica@polymer microspheres is observed by TEM. Besides, under nitrogen the organic layer decomposition of carbonaceous residue possibly remains on the silica material [11], which makes a lower theoretical content of the coated polymer and therefore a lower thickness.

The chemical composition of the coated polymer in the silica@polymer microspheres is detected by FT-IR. Fig. 3 shows the FT-IR spectra of the silica microspheres before and after polymer coating. Due to the low content of the coated polymer in the silica@polymer microspheres, the FT-IR spectra of the silica microspheres before and after polymer being coated are very similar. However, as indicated by the inset in Fig. 3, the characteristic absorption at ~1700 cm^{-1} ascribed to the carbonyl group in the PAEMA segment can be clearly observed, indicating the success of the polymer coating on the silica microspheres.

The chemical composition of the coated polymer in the silica@polymer microspheres is further detected by ^{13}C CPMAS NMR. Fig. 4 shows the solid state ^{13}C CPMAS NMR spectra of the silica@polymer microspheres. As indicated by the inset in Fig. 4, the characteristic chemical shifts due to the polystyrene (PS) and PAEMA segments are well recorded, confirming the chemical composition of the coated polymer. Herein, it should be noted that readers can refer the ^{13}C CPMAS NMR spectra of the corresponding polymers as introduced elsewhere [51].

3.2. Immobilization and characterization of noble metal nanoparticles on the polymer coated silica microspheres of silica@polymer

PAEMA is a typical coordinate polymer, which contains the chelate ligand of β-diketone and has been used as scaffold for transitional metal catalyst [46–48]. Therefore, when $PdCl_2$ is added into the aqueous dispersion of the silica@polymer microspheres, Pd ions are initially coordinated with the chelate ligand of β-diketone and then the Pd nanoparticles are immobilized on the silica@polymer microspheres by reducing with $NaBH_4$ aqueous solution.

To evaluate the catalyst loading capacity of the silica@polymer microspheres, different amount of $PdCl_2$ is added into a given volume of the aqueous dispersion of the silica@polymer microspheres to coordinate with the chelate ligand of β-diketone for 2 h and then is reduced with $NaBH_4$ aqueous solution. It is found that the catalyst loading capacity of the silica@polymer microspheres is dependent on the molar ratio of the coordinate PAEMA segment to the Pd precursor. As shown in Fig. 5A, when the molar ratio of the corresponding AEMA to $PdCl_2$ is 1:1, most of the resultant Pd nanoparticles are located outside the silica@polymer microspheres. When the ratio increases to 2:1, the immobilization of Pd nanoparticles on the silica@polymer microspheres is greatly improved as shown in Fig. 5B. When the ratio increases

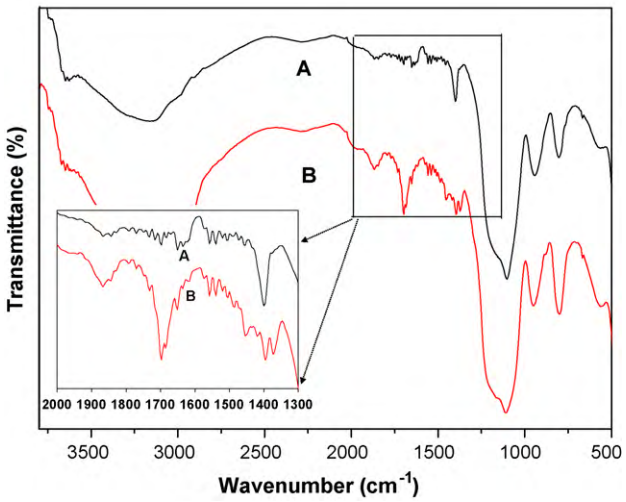

Fig. 3. FT-IR spectra of the silica microspheres (A) and the silica@polymer microspheres (B).

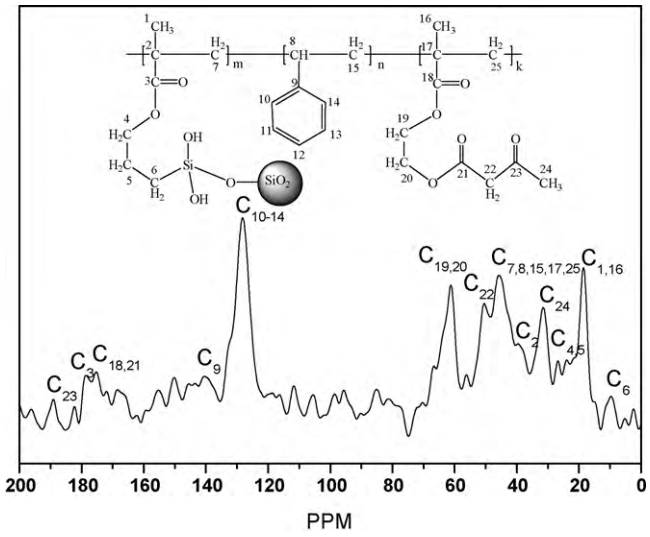

Fig. 4. Solid state ^{13}C CPMAS NMR spectra of the silica@polymer microspheres.

to 4:1, almost all the resultant Pd nanoparticles are immobilized on the silica@polymer microspheres (Fig. 5C). When the ratio further increases to 8:1, no free Pd nanoparticles but immobilized Pd nanoparticles on the silica@polymer microspheres can be observed (Fig. 5D). Under the optimized molar ratio of AEMA/Pd at 8:1, the catalyst loading capacity is 0.19 mmol Pd per gram of silica@polymer microspheres. From Fig. 5D, it is clearly discerned that the Pd nanoparticles are uniformly dispersed on the surface of the silica@polymer microspheres. From the size dispersion shown in Fig. 6, the average size of the immobilized Pd nanoparticles, 5.1 nm, is calculated.

To evaluate the role of the coated polymer on immobilization of Pd nanoparticles, silica microspheres without coated polymer layer is checked. As shown in Fig. 7, no Pd nanoparticles immobilized on the silica microspheres is observed. This result suggests that the coated polymer of PS-*co*-PAEMA plays a key role in the immobilization of Pd nanoparticles on silica microspheres. Furthermore, as discussed elsewhere [52], unfunctionalized polystyrene material is

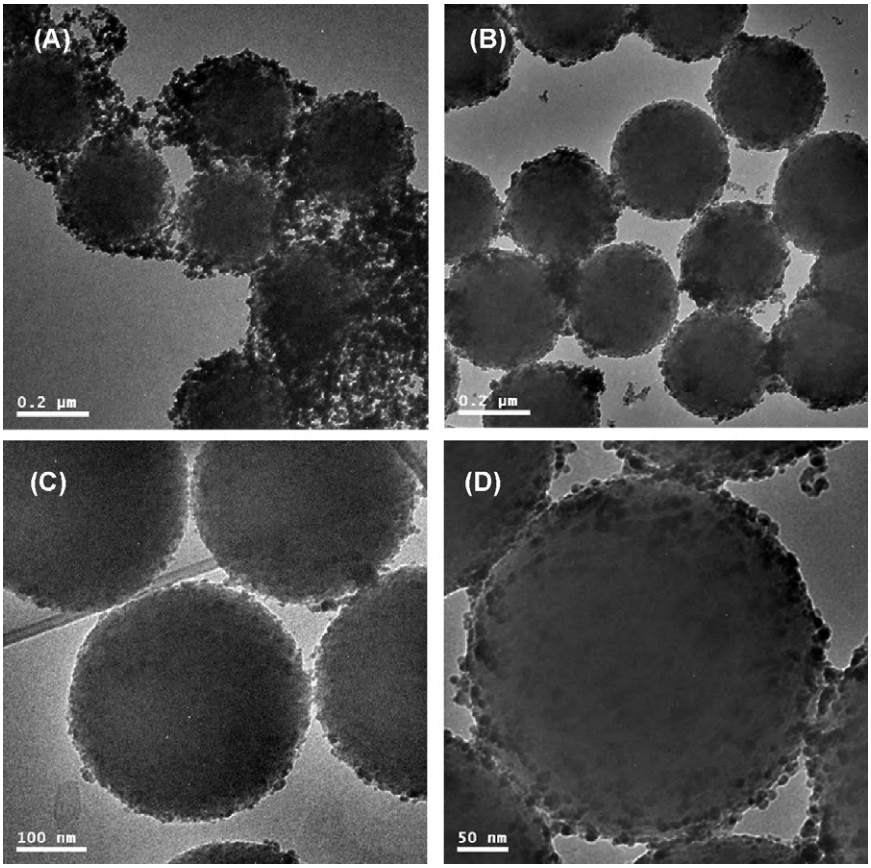

Fig. 5. TEM images of Pd nanoparticles immobilized on the silica@polymer microspheres, in which the Pd particles are synthesized with the molar ratio of AEMA/Pd at 1:1 (A), 2:1 (B), 4:1 (C) and 8:1 (D), respectively.

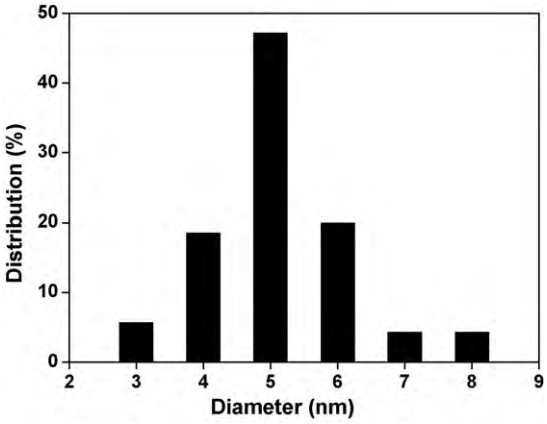

Fig. 6. Size distribution of the Pd nanoparticles immobilized on the silica@polymer microspheres synthesized with the molar ratio of AEMA/Pd at 8:1.

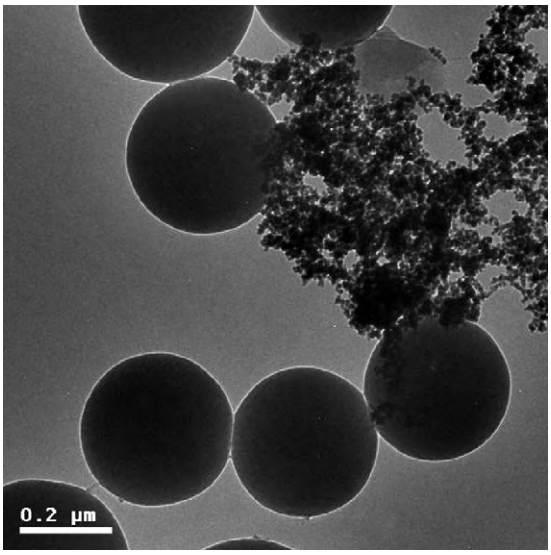

Fig. 7. TEM image of Pd nanoparticles synthesized in the presence of the silica microspheres without coating polymer.

not a suitable scaffold for immobilization of noble metal nanoparticles. Therefore, we conclude that the present immobilization of Pd nanoparticles is ascribed to the chelate ligand of β-diketone in the PAEMA segment in the coated polymer layer.

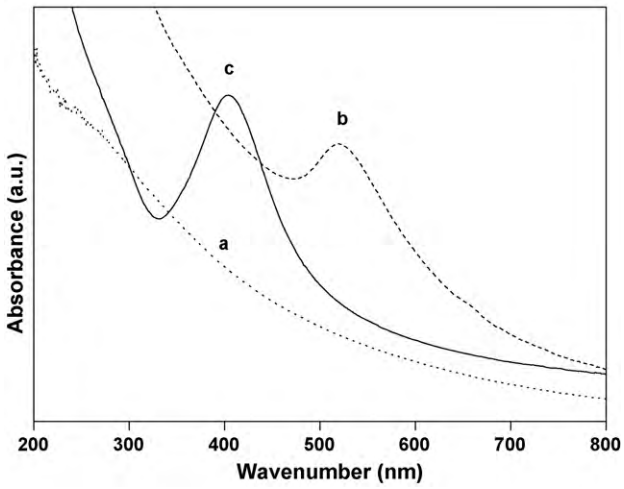

Fig. 9. UV–vis spectra of the aqueous dispersion of Pd/silica@polymer (a), Au/silica@polymer (b) and Ag/silica@polymer (c).

Besides Pd nanoparticles, Au and Ag nanoparticles can also be immobilized on the silica@polymer microspheres with the molar ratio of AEMA to the metal precursors at 8/1. Fig. 8 shows the TEM images of the Au and Ag nanoparticles immobilized on the silica@polymer microspheres. Clearly, the *in situ* synthesized Au and Ag nanoparticles, the average sizes of which are 6.1 and 5.7 nm, are uniformly dispersed on the silica@polymer microspheres.

It is well documented that UV–vis spectroscopy can be used to diagnose the aggregation state of noble metal nanoparticles [53,54]. For example, highly dispersed 5–20 nm Au nanoparticles exhibit an absorbance peak at ~520 nm. As the Au particle size decreases, hypsochromic shift of the characteristic absorbance occurs, and no sharp absorbance peak is observed within the UV–vis range when the size of Au nanoparticles further decreases to less than 3 nm. Fig. 9 shows the UV–vis spectra of Pd, Au and Ag nanoparticles immobilized on the silica@polymer microspheres. Similar to the platinum-group metal nanoparticles [55], no characteristic absorption peak but just a broad continuous absorption in the UV–vis range is observed for the immobilized Pd nanoparticles. Whereas the distinct absorption peaks around 520 nm for the immobilized Au nanoparticles and 420 nm for the immobilized Ag nanoparticlesc are clearly observed, indicating formation of ~5 nm Au and ~5 nm Ag nanoparticles on the silica@polymer microspheres.

The noble metal nanoparticles immobilized on the silica@polymer microspheres are further characterized by XRD. The XRD patterns of the Pd nanoparticles immobilized on the

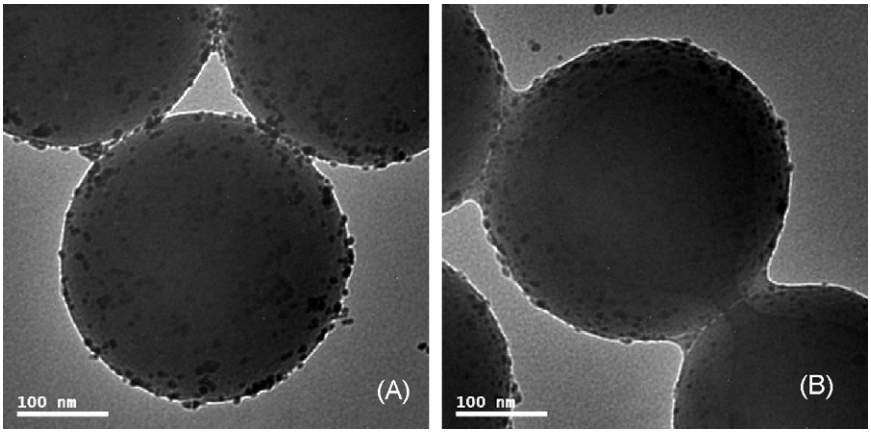

Fig. 8. TEM images of the Au/silica@polymer (A) and the Ag/silica@polymer (B) synthesized with the molar ratio of AEMA to the metal precursors at 8/1.

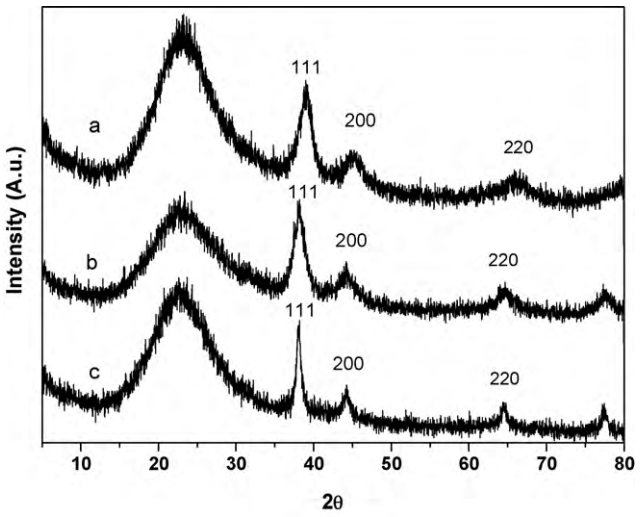

Fig. 10. XRD pattern of Pd/silica@polymer (a), Au/silica@polymer (b) and Ag/silica@polymer (c).

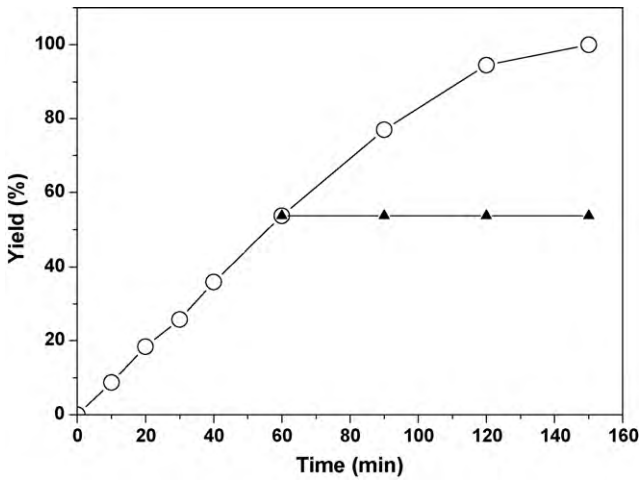

Fig. 11. Time-dependent yield of hydrocinnamic alcohol for the hydrogenation reaction of cinnamyl alcohol in water at 27 °C in the presence of 0.20 mol% Pd/silica@polymer catalyst (○) and after removal of the Pd/silica@polymer catalyst (▲).

silica@polymer microspheres shown in Fig. 10 display three diffraction peaks at 2θ of 38.9°, 45.2°, and 66.2°, corresponding to the diffraction of the (1 1 1), (2 0 0), and (2 2 0) lattice planes of the face-centered cubic structure of Pd nanoparticles. Furthermore, the broad diffraction with 2θ ranging from 12 to 35° ascribed to the silica@polymer microspheres can also be clearly observed. In terms of the Scherrer's equation [56], using the diffraction peak of (1 1 1) lattice plane of the Pd nanoparticles, the average size of the Pd nanoparticles is calculated to be 5.2 nm, which is well consistent with that observed with TEM. The XRD patterns of the Au and Ag nanoparticles immobilized on the silica@polymer microspheres shown in Fig. 10 also reveal three diffraction peaks at 2θ of 38.1°, 44.0°, 64.6° and 38.1°, 44.2°, 64.5° corresponding to the diffraction of (1 1 1), (2 0 0), and (2 2 0) lattice planes of the face-centered cubic structure of Au and Ag nanoparticles. Similarly, the Au nanoparticles size of 5.8 nm and Ag nanoparticles size of 10.2 nm are calculated.

3.3. Catalyst testing

Herein the typical catalyst of the Pd nanoparticles immobilized on the silica@polymer microspheres, Pd/silica@polymer, is tested using the hydrogenation of cinnamyl alcohol at 300 K in water as model reaction, in which hydrocinnamic alcohol is the only resultant product. Fig. 11 shows the time-dependent yield of hydrocinnamic alcohol in water at 27 °C. The yield almost linearly increases with time to 77% in 90 min, and in the next 60 min almost quantitive yield is achieved. The Pd/silica@polymer catalyst affords a turnover frequency (TOF) value of 270 h^{-1} in the hydrogenation of cinnamyl alcohol at 300 K in water, which is measured as moles of product per molar Pd per hour in the initial hydrogenation.

The Pd leaching into aqueous phase at the reaction temperature is further checked. After the yield of hydrocinnamic alcohol reaches to 54% in 60 min, the Pd/silica@polymer catalyst was initially filtered off at the reaction temperature of 27 °C. Then, the liquid phase of the filtrate containing the reactant of cinnamyl alcohol was bubbled with H_2 at 27 °C. As shown in Fig. 11, no further yield of hydrocinnamic alcohol is observed in the next 90 min. AAS analysis also confirms that no Pd catalyst is leached into the filtrate and the Pd content in the collected recycled catalyst is almost as same as those in the fresh Pd/silica@polymer catalyst. These results demonstrate that the Pd catalyst leaching in the present reaction condition is very slightly.

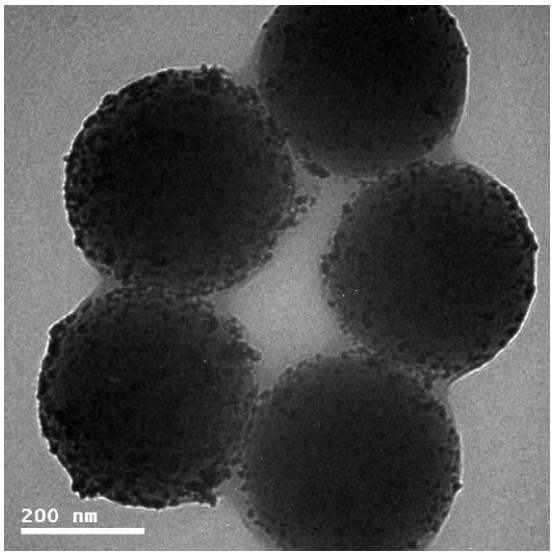

Fig. 12. TEM image of the recycled Pd/silica@polymer catalyst.

The recycling of the Pd/silica@polymer catalyst is further studied. Since both the PS and PAEMA segments are hydrophobic, the surface of the silica@polymer microspheres is deemed to be hydrophobic, which makes separation of the Pd/silica@polymer catalyst from the reaction mixture relatively easy. It is found that the Pd/silica@polymer catalyst exists as suspending powder when the reaction mixture is stirred. When the reaction mixture is not stirred anymore, the Pd/silica@polymer catalyst exists as fine precipitate. This allows a complete separation of the catalyst from the reaction mixture by filtration and convenient reuse of the catalyst. In fact, it was found that the yield remained more or less same (~99%) even after eight cycles of hydrogenation as shown in Table 1.

The recycled Pd/silica@polymer catalyst is further characterized by TEM. As shown in Fig. 12, it is clearly observed that the size and morphology of the silica@polymer microspheres remains unchanged, suggesting the stability of the silica@polymer microspheres. Furthermore, the size of Pd nanoparticles in the recycled Pd/silica@polymer catalyst is almost as same as those in the fresh one and no conglomeration of Pd nanoparticles is observed after eight cycles of hydrogenation, which confirms the good reusability of the Pd/silica@polymer catalyst.

Table 1
Recycling of the Pd/silica@polymer catalyst in the hydrogenation reaction of cinnamyl alcohol in water.[a]

	Run							
	1st	2nd	3rd	4th	5th	6th	7th	8th
Yield[b] (%)	>99	>99	>99	>99	>99	>99	>99	>99

[a] Reaction conditions: cinnamyl alcohol (2.0 mmol) and 15.0 mL of aqueous dispersion containing 0.20 mol% Pd/silica@polymer catalyst (in the 1st run), 27 °C, 2.5 h.
[b] Isolated yield and the purity of isolated product was confirmed by ^{1}H NMR.

4. Conclusions

A strategy to immobilize noble metal nanoparticles on silica microspheres is introduced. Following this strategy, 350 nm silica microspheres, which are produced through hydrolysis of tetraethylorthosilicate according to the Stöber method, are initially activated with 3-(trimethoxysilyl) propyl methacrylate to anchor C=C bonds on the surface of the silica microspheres. Then a thin layer of the cross-linked coordination polymer of PS-*co*-PAEMA is coated on the surface of the activated silica microspheres by dispersion polymerization of styrene and AEMA in the presence of the PVP stabilizer. The noble metal nanoparticles therefore can be immobilized on the polymer coated silica microspheres initially through coordination between the chelate ligand of β-diketone in the coated polymer and metal precursors followed by reduction. It is confirmed that the immobilization of noble metal nanoparticles on silica microspheres is ascribed to the chelate coated polymer. That is, without the chelate coated polymer, noble metal nanoparticles cannot be immobilized on silica microspheres. And furthermore, the amount of immobilized catalyst is dependent on the ratio of the chelate ligand of β-diketone to the metal precursor. When the molar ratio is 8/1, it is found that the catalyst of 5.1 nm Pd, 6.1 nm Au, and 5.7 nm Ag nanoparticles can be favorably immobilized on the polymer coated silica microspheres. The typical catalyst of the Pd nanoparticles immobilized on the polymer coated silica microspheres is tested using hydrogenation of cinnamyl alcohol in water at 300 K as model reaction. The catalysis demonstrates that the immobilized Pd catalyst affords a TOF value of 270 h^{-1}, and no catalyst leaching into aqueous phase is detected, and the immobilized Pd catalyst can be reused at least eight times without loss of catalytic activity.

Acknowledgements

The financial support by National Science Foundation of China (No. 20974051), Tianjin Natural Science Foundation (No. 09JCYBJC02800), and the Program for New Century Excellent Talents in University (No. NCET-06-0216) is gratefully acknowledged.

Appendix A. Supplementary data

Supplementary data associated with this article can be found, in the online version, at doi:10.1016/j.molcata.2010.05.018.

References

[1] A. Roucoux, J. Schulz, H. Patin, Chem. Rev. 102 (2002) 3757.
[2] M.F. Williams, B. Fonfé, C. Woltz, A. Jentys, J.A.R. van Veen, J.A. Lercher, J. Catal. 251 (2007) 497.
[3] S. Bernal, J.J. Calvino, M.A. Cauqui, J.M. Gatica, C. Larese, J.A. Perez Omil, J.M. Pintado, Catal. Today 50 (1999) 175.
[4] A.M. Caporusso, P. Innocenti, L.A. Aronicaa, G. Vitulli, R. Gallina, A. Biffis, M. Zecca, B. Corain, J. Catal. 234 (2005) 1.
[5] (a) A. Biffis, L. Minati, J. Catal. 236 (2005) 405;
(b) D.I. Svergun, E.V. Shtykova, A.T. Dembo, L.M. Bronstein, O.A. Platonova, A.N. Yakunin, P.M. Valetsky, A.R. Khokhlov, J. Chem. Phys. 109 (1998) 11109;
(c) X. Jiang, D. Xiong, Y. An, P. Zheng, W. Zhang, L. Shi, J. Polym. Sci., A: Polym. Chem. 45 (2007) 2812.
[6] (a) V.G. Pol, H. Grisaru, A. Gedanken, Langmuir 21 (2005) 3635;
(b) L. Cen, K.G. Neoh, E.-T. Kang, Adv. Mater. 17 (2005) 1656;
(c) J.L. Ou, C.P. Chang, Y. Sung, K.L. Ou, C.C. Tseng, H.W. Ling, M.D. Ger, Colloids Surf. A 305 (2007) 36;
(d) H.S. Mohammed, D.A. Shipp, Macromol. Rapid Commun. 27 (2006) 1774;
(e) Y. Zhu, C.N. Lee, R.A. Kemp, N.S. Hosmane, J.A. Maguire, Chem. Asian J. 3 (2008) 650;
(f) G. Sharma, Y. Mei, Y. Lu, M. Ballauff, T. Irrgang, S. Proch, R. Kempe, J. Catal. 246 (2007) 10;
(g) Y. Mei, Y. Lu, F. Polzer, M. Ballauff, M. Drechsler, Chem. Mater. 19 (2007) 1062.
[7] (a) G.G. Wildgoose, C.E. Banks, R.G. Compton, Small 2 (2006) 182;
(b) Q. Liu, Z.-M. Cui, Z. Ma, S.-W. Bian, W.-G. Song, J. Phys. Chem. C 112 (2008) 1199;
(c) X. Chen, Y. Hou, H. Wang, Y. Cao, J. He, J. Phys. Chem. C 112 (2008) 8172.
[8] (a) J. Zeng, J. Yang, J.Y. Lee, W. Zhou, J. Phys. Chem. B 110 (2006) 24606;
(b) S. Domínguez-Domínguez, A. Berenguer-Murcia, B.K. Pradhan, A. Linares-Solano, D. Cazorla-Amoros, J. Phys. Chem. C 112 (2008) 3827;
(c) E.P. Maris, W.C. Ketchie, M. Murayama, R.J. Davis, J. Catal. 251 (2007) 281.
[9] Y. Xie, S. Quinlivan, T. Asefa, J. Phys. Chem. C 112 (2008) 9996.
[10] A. Barau, V. Budarin, A. Caragheorgheopol, R. Luque, D.J. Macquarrie, A. Prelle, V.S. Teodorescu, M. Zaharescu, Catal. Lett. 124 (2008) 204.
[11] P. Centomo, M. Zecca, B. Corain, J. Cluster Sci. 18 (2007) 947.
[12] Y. Jiang, Q. Gao, J. Am. Chem. Soc. 128 (2006) 716.
[13] (a) T. Matsumoto, M. Ueno, N. Wang, S. Kobayashi, Chem. Asian J. 3 (2008) 239;
(b) M. Kralik, V. Kratky, P. Centomo, P. Guerriero, S. Lora, B. Corain, J. Mol. Catal. A: Chem. 195 (2003) 219.
[14] Z. Chen, T. Gang, K. Zhang, J. Zhang, X. Chen, Z. Sun, B. Yang, Colloids Surf. A: Physicochem. Eng. Aspects 272 (2006) 151.
[15] X. Zhou, T. Wu, B. Hu, T. Jiang, B. Han, J. Mol. Catal. A: Chem. 306 (2009) 143.
[16] L. Huang, Z. Wang, T.P. Ang, J. Tan, P.K. Wong, Catal. Lett. 112 (2006) 219.
[17] S. Chytil, W.R. Glomm, E. Vollebekk, H. Bergem, J. Walmsley, J. Sjöblom, E.A. Blekkan, Micropor. Mesopor. Mater. 86 (2005) 198.
[18] Y. Chen, C. Wang, H. Liu, J. Qiu, X. Bao, Chem. Commun. (2005) 5298.
[19] H.G. Zhu, C.D. Liang, W.F. Yan, S.H. Overbury, S. Dai, J. Phys. Chem. B 110 (2006) 10842.
[20] H.J. Shin, R. Ryoo, Z. Liu, O. Terasaki, J. Am. Chem. Soc. 123 (2001) 1246.
[21] Y.J. Han, J.M. Kim, G.D. Stucky, Chem. Mater. 12 (2000) 2068.
[22] A. Fukuoka, H. Araki, J. Kimura, Y. Sakamoto, T. Higuchi, N. Sugimoto, S. Inagaki, M. Ichikawa, J. Mater. Chem. 14 (2004) 752.
[23] A. Fukuoka, Y. Sakamoto, S. Guan, S. Inagaki, N. Sugimoto, Y. Fukushima, K. Hirahara, S. Iijima, M. Ichikawa, J. Am. Chem. Soc. 123 (2001) 3373.
[24] P. Karwiec, E. Kockrick, P. Simon, G. Auffermann, S. Kaskel, Chem. Mater. 18 (2006) 2663.
[25] A.K. Prashar, R.P. Hodgkins, R. Kumar, R.N. Devi, J. Mater. Chem. 18 (2008) 1765.
[26] J.R. Agger, M.W. Anderson, M.E. Pemble, O. Terasaki, Y. Nozue, J. Phys. Chem. B 102 (1998) 3345.
[27] H. Parala, H. Winkler, M. Kolbe, A. Wohlfart, R.A. Fischer, R. Schmechel, H. Von Seggern, Adv. Mater. 12 (2000) 1050.
[28] K.-B. Lee, S.-M. Lee, J. Cheon, Adv. Mater. 13 (2001) 517.
[29] G. Gupta, P.S. Shah, X. Zhang, A.E. Saunders, B.A. Korgel, K.P. Johnston, Chem. Mater. 17 (2005) 6728.
[30] R.M. Rioux, H. Song, J.D. Hoefelmeyer, P. Yang, G.A. Somorjai, J. Phys. Chem. B 109 (2005) 2192.
[31] Y. Guari, C. Thieuleux, A. Mehdi, C. Reye, R.J.P. Corriu, S. Gomez-Gallardo, K. Philippot, B. Chaudret, R. Dutartre, Chem. Commun. (2001) 1374.
[32] C.M. Yang, P.H. Liu, Y. Ho, C. Chiu, K. Chao, Chem. Mater. 15 (2003) 275.
[33] C.S. Gill, B.A. Price, C.W. Jones, J. Catal. 251 (2007) 145.
[34] R.B. Bedford, U.G. Singh, R.I. Walton, R.T. Williams, S.A. Davis, Chem. Mater. 17 (2005) 701.
[35] (a) K. Shimizu, S. Koizumi, T. Hatamachi, H. Yoshida, S. Komai, T. Kodama, Y. Kitayama, J. Catal. 228 (2004) 141;
(b) S. Tandukar, A. Sen, J. Mol. Catal. A: Chem. 268 (2007) 112.
[36] L.X. Zhang, J.L. Shi, J. Yu, Z.L. Hua, X.G. Zhao, M.L. Ruan, Adv. Mater. 14 (2002) 1510.
[37] (a) T. Ribeiro, C. Baleizao, J.P.S. Farinha, J. Phys. Chem. C 113 (2009) 18082;
(b) G. Liu, H. Zhang, X. Yang, Y. Wang, Polymer 48 (2007) 5896;
(c) P. Jiang, M.J. McFarland, J. Am. Chem. Soc. 126 (2004) 13778.
[38] Z. Zeng, J. Yu, Z.-X. Guo, Macromol. Chem. Phys. 205 (2004) 2197.
[39] S. Gu, T. Kondo, M. Konno, J. Colloid Interface Sci. 272 (2004) 314.
[40] K. Zhang, H. Chen, X. Chen, Z. Chen, Z. Cui, B. Yang, Macromol. Mater. Eng. 288 (2003) 380.
[41] R. Atkin, M. Bradley, B. Vincent, Soft Matter 1 (2005) 160.
[42] (a) N. Sheibat-Othman, E. Bourgeat-Lami, Langmuir 25 (2009) 10121;
(b) H. Zhang, Z. Su, P. Liu, F. Zhang, J. Appl. Polym. Sci. 104 (2007) 415.

[43] (a) S. Reculusa, C. Poncet-Legrand, S. Ravaine, C. Minogotaud, E. Duguet, E. Bourgeat-Lami, Chem. Mater. 14 (2002) 2354;
(b) A. Schmid, S. Fujii, S.P. Armes, C.A.P. Leite, F. Galembeck, H. Minami, N. Saito, M. Okubo, Chem. Mater. 19 (2007) 2435;
(c) X. Cheng, M. Chen, S. Zhou, L. Wu, J. Polym. Sci. A: Polym. Chem. 44 (2006) 3807.
[44] W. Stöber, A. Fink, E. Bohn, J. Colloid Interface Sci. 26 (1968) 62.
[45] S. Kawaguchi, K. Ito, Adv. Polym. Sci. 175 (2005) 299.
[46] (a) P. Zheng, W. Zhang, J. Catal. 250 (2007) 324;
(b) Y. Lan, M. Zhang, W. Zhang, L. Yang, Chem. Eur. J. 15 (2009) 3670.
[47] T. Kaliyappan, P. Kannan, Prog. Polym. Sci. 25 (2000) 343.
[48] T. Krasia, R. Soula, H.G. Börner, H. Schlaad, Chem. Commun. (2003) 538.
[49] H. Zou, S. Wu, J. Shen, Chem. Rev. 108 (2008) 3893.
[50] Y. Zhang, Q. Zhou, S. Chen, P. Dong, G. Yuan, CIESC J. 60 (2009) 1327.
[51] (a) C.A. Quirarte-Escalante, V. Soto, W. Cruz, G.R. Porras, R. Manríquez, S. Gomez-Salazar, Chem. Mater. 21 (2009) 1439;
(b) M. Zhang, W. Zhang, J. Phys. Chem. C 112 (2008) 6245.
[52] X.W. Lou, C. Yuan, E. Rhoades, Q. Zhang, L.A. Archer, Adv. Funct. Mater. 16 (2006) 1679.
[53] P.B. Johnson, R.W. Christy, Phys. Rev. B 6 (1972) 4370.
[54] A.C. Templeton, J.J. Pietron, R.W. Murray, P. Mulvaney, J. Phys. Chem. B 104 (2000) 564.
[55] (a) N. Toshima, T. Takahashi, Bull. Chem. Soc. Jpn. 65 (1992) 400;
(b) N. Toshima, K. Kushihashi, T. Yonezawa, H. Hirai, Chem. Lett. (1989) 1769;
(c) T. Teranishi, M. Miyake, Chem. Mater. 10 (1998) 594.
[56] H.P. Klug, L.E. Alexander, X-ray Diffraction Procedures, Wiley, New York, 1959.